Graphene oxide modified semi-aromatic polyamide thin film composite membranes for PPCPs removal

Jue Wang[a,b], Nana Li[a,b], Yu Zhao[a], Shengji Xia[a,b],*

[a]*State Key laboratory of Pollution Control and Resources Reuse, Tongji University, Shanghai, 200092, China,*
email: xiashengji@tongji.edu.cn (S. Xia), 942586423@qq.com (Y. Zhao)
[b]*Key laboratory of Yangtze River Water Environment, Ministry of education, Tongji University, Shanghai, 200092, China,*
email: 1432829linana@tongji.edu.cn (N. Li)

ABSTRACT

The incorporation of nano-materials in thin film composite (TFC) membrane has been explored in order to improve permeability/selectivity and to enhance anti-fouling properties in many water treatment processes. In this study, graphene oxide (GO) was embedded into the semi-aromatic polyamide active layer of a TFC membrane via interfacial polymerization (IP) reaction between the piperazine (PIP) and trimesoyl chloride (TMC) monomers. The properties of TFC membranes were thoroughly characterized using FTIR, FE-SEM, AFM, and water contact angle measurements. The permeation and separation performance of these membranes were also examined. The in-house fabricated PA/GO TFC membranes exhibited much higher flux (12.78 ± 0.36 L/m²·h·bar) than that of the pristine PA TFC membranes (8.94 ± 0.42 L/m²·h·bar) with a slightly increased salt rejection. Furthermore, the rejection of three target PPCPs compounds, i.e., paracetamol, norfloxacin and sulfamethoxazole was investigated using these TFC membranes with different GO loadings. The addition of GO offered a significant improvement in PPCPs rejection as a result of favorable change in membrane hydrophilicity, surface morphology and surface charge. This study offers a facile and effective route to fabricate high performance semi-aromatic PA TFC membranes incorporated with functional nano-materials.

Keywords: Graphene oxide; Semi-aromatic polyamide membrane; Thin film composite; Interfacial polymerization; PPCPs

1. Introduction

Since the concept of interfacial polymerization (IP) was first introduced by Morgan et al. in 1965 [1], fabricating thin-film composite (TFC) membranes via this approach has experienced a tremendous growth and are widely used nowadays in nanofiltration (NF) and reverse osmosis (RO) processes for water treatment [2–4]. NF, as a promising membrane technology, plays an active role in waste water treatment, seawater desalination, ion separation, and solvents purification, due to its capability of removing a broad range of contaminants in a single treatment step with high water flux and low operation pressure compared with the RO process.

A typical TFC nanofiltration (TFC–NF) membrane consists three layers: a non-woven fabric layer for mechanical strength, a microporous polysulfone support layer, and a thin top selective polyamide layer [5,6]. The material used in the top layer-polyamide (PA) can be roughly categorized in two types: fully aromatic PA (aromatic amine monomers brought into contact with aromatic acid chloride monomers by interfacial polymerization) and semi-aromatic PA (aliphatic amine monomers brought into contact with aromatic acid chloride monomers by interfacial polymerization). The semi-aromatic PA TFC membrane usually has a lower membrane surface roughness than the fully aromatic membrane, at the same time appears to be more hydrophilic and permeable [7]. However, the semi-aromatic membrane appears to be less selective and have lower salt rejection (NaCl rejection: 21.3~56.9%) than the

_____

*Corresponding author.

fully aromatic membrane (NaCl rejection: 91.5~96.5%) [8]. Meanwhile the issues associated with fouling also impede its further advance in industrial implementation. The efficiency of membrane technology can be greatly enhanced by using the membranes with high permeability and good rejection. Numerous researches have been focused on optimizing the ultra-thin active layer in an attempt to improve the performance of the PA TFC membranes, including the introduction of new monomers [9,10], surfactant [11] and nanoparticles [3] in the IP process. The nanoparticles that have been explored so far included nano-TiO_2 [12], nano-silver [13], carbon nanotubes [14] and graphene oxide (GO) [15].

Graphene oxide nano-sheet is a one-atom-layer-thick two-dimensional carbon sheet, which has attracted increasing attentions for a new generation of applications based on carbon nano-materials [16]. GO has been hyped as a super material with impressive properties such as high surface area, prominent electron transport, great mechanical properties and superior hydrophilicity [17]. Recently, the water permeability of a graphene oxide membrane was described [18,19], which opened a new horizon for water desalination and separation of organic foulant [20–22]. In addition, modifying membranes with GO could potentially achieve superior hydrophilicity, outstanding selectivity and excellent antifouling properties due to the presence of oxygen-containing functional groups in graphene oxide [20,23,24].

Many research efforts have been dedicated to GO modified fully aromatic PA TFC membranes aiming for superior membrane performance. Francois et al. conferred strong antimicrobial properties to thin-film composite polyamide membranes by a simple graphene oxide surface functionalization, which offered a promising approach for novel antimicrobial membranes [21]. Kim et al. showed that the GO functionalized polyamide membranes displayed considerably improved performances, such as water flux, chlorine resistance and radical scavenging ability [25]. A novel GO modified TFC membrane prepared by Bano et al. exhibited excellent hydrophilicity, desired surface charge and decreased surface roughness, all of which led to a higher water flux, stable salt rejection and outstanding anti-fouling properties [26]. However, to the best knowledge of the authors, only a handful of studies have focused on the incorporating of GO nano-materials with semi-aromatic PA TFC membranes.

Pharmaceuticals and personal care products (PPCPs) being released into the aquatic environment present a potential risk to human health and environmental implications. It is therefore essential to implement advanced treatment technologies such as membrane processes to remove PPCPs from treated effluent before entering the aquatic environment as well as water reuse [27–31]. Three PPCPs, namely, paracetamol, norfloxacin and sulfamethoxazole are among the few pollutants posing the most threat due to their widespread use as analgesic/antipyretic, medication of antibacterial, and antibiotic [32].
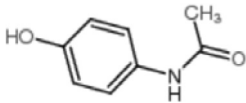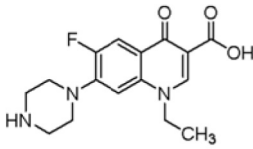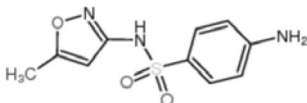
In this study, the GO modified semi-aromatic PA TFC membranes with different GO loadings were prepared via the IP process using PIP (piperazine) and TMC (trimesoyl chloride) on the PSf UF membrane substrates for the removal of three target PPCPs compounds: paracetamol, norfloxacin and sulfamethoxazole. Fourier transform infrared spectroscopy (FTIR), field emission scanning electron microscopy (FE-SEM)，atomic force microscope (AFM) and water contact angle tests were utilized to evaluate the composition, structure and hydrophilicity of the membrane. The water permeation performance, salt rejection and PPCPs removal efficiency of these membranes were also systematically investigated.

2. Experimental

2.1. Materials

Graphene oxide nano-sheets were purchased from Sigma Aldrich. The apparent thickness of GO sheet was approximately 1 nm, with the lateral dimensions ranging from a few nanometers to hundreds of micrometers. PSf UF membrane (molecular weight cut-off: 100 kDa) was obtained from XINLIMO Tech Co., Ltd., China. Piperazine (PIP) with 99% purity and 1, 3, 5-benzenetricarbonyl trichloride (TMC) purchased from Sigma Aldrich were used as interfacial reaction monomer. M-hexane (Sinopharm Chemical Reagent Co., Ltd, China) was used as the solvent. Deionized (DI) water (18.2 MΩ cm at 25°C) was provided by a water purification system (Milli-Q, Millipore Corporation, USA) and used in solution preparation and membrane washing. Paracetamol, norfloxacin and sulfamethoxazole (Aladdin) were selected as the target compounds. The detailed properties of these three compounds are shown in Table 1.

Table 1
Characteristics of the organic compounds

Target compound	CAS Number	Molecular formula	Chemical structural formula	Molecular weight
Paracetamol	103-90-2	$C_8H_9NO_2$		151.16
Norfloxacin	70458-96-7	$C_{16}H_{18}FN_3O_3$		319.33
Sulfamethoxazole	723-46-6	$C_{10}H_{11}N_3O_3S$		253.28

2.2. Membrane preparation

PIP-TMC TFC membranes with different GO loadings in the top layer were prepared via the IP reaction. The fabrication process of membranes was showed in Fig. 1. Prior to use, GO nano-sheets were dispersed into deionized water by sonication for 20 min to form a 0.1 wt% suspension solution. PSf UF membranes were immersed in DI water for 24 h before use. Different volumes of 0.1 wt% GO suspension solution were added into 1% (w/v) PIP aqueous solution to form solutions with different GO concentrations (0, 0.004, 0.008 and 0.016 wt%). The aqueous solution containing PIP/GO was poured onto the membrane surface with sonication for 2 min, and then the excess solution was removed from the membrane surface using a rubber roller. After drying in air for 1 min, 0.1% (w/v) TMC solution in m-hexane was poured onto the membrane, and kept for 1 min to form PA layer via the IP reaction. The unreacted PIP and TMC were removed from membrane surface by rinsing the membrane with the m-hexane. The membrane was then soaked in 0.2% (w/v) sodium carbonate solution for 5 min and was thermally treated in a vacuum oven at 60°C for 8 min. All the membrane samples were stored in DI water prior to further testing.

2.3. Membrane characterization

2.3.1. Surface hydrophobicity

The dynamic water contact angle was measured using an optical tension meter (Attension Theta Lite, Biolin Scientific Co. Ltd., Sweden). Deionized water droplets from a micro-syringe with a stainless steel needle were dropped on the dry membrane surface. A reliable contact angle value was acquired by averaging 5 measurements of different positions of the membrane surface.

2.3.2. Surface charge

A streaming potential instrument (SurPASS, Anton Paar, Austria) was utilized to examine the zeta potentials of membranes at 25.0 ± 0.5°C in 1.0 mM KCl solution over the pH range of 5–11.

2.3.3. Morphology and microstructure

The top surface and cross-section micromorphology of the in-house fabricated membranes were observed by field-emission scanning electron microscope (FE-SEM, Ultra 55, Carl Zeiss company, Germany) operated under standard high-vacuum conditions at 5.00 kV. Before analysis, samples were air-dried and sputtered with a thin gold layer.

Atomic force microscopy (AFM) was utilized to analyze the membrane surface morphology and roughness using the scanning probe microscope (Multimode 8, Bruker Corporation, USA).

2.3.4. Chemistry properties

The surface chemistry and composition of the TFC membranes were analyzed by attenuated total reflectance-fourier transform infrared spectroscopy (ATR-FTIR, Nicolet iS5, Thermo Fisher Scientific Inc, USA). ATR-FTIR analyses were carried out with a Ge crystal as background over the wavenumber range of 800–4000 cm^{-1}.

2.3.5. Surface carboxyl group density

The carboxyl group density on the TFC membrane surface was quantified via the Toluidine Blue O (TBO) technique developed by Tiraferri et al. [33] The support layer of the TFC membrane was sealed with waterproof tape to expose the membrane active layer. Then, this active layer was in contact with a freshly prepared solution of TBO (2 mM) and NaOH (pH 11), and reacted with the positively charged TBO molecules to deprotonated carboxylic acid groups on the polyamide surface. The membrane was rinsed with a dye-free NaOH solution (pH 11) to remove all the unbound dye molecules, and afterwards immersed into a NaCl solution at pH 2 to elute the bonded TBO dye from the polyamide surface. The ultraviolet spectrophotometer at a 630 nm wavelength was used to measure the absorbance of the eluent for determining the surface carboxyl group density.
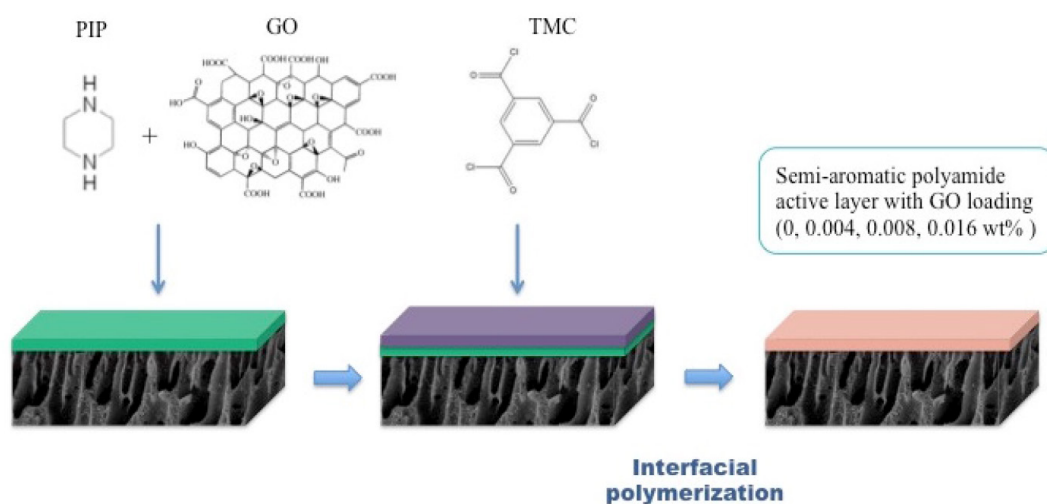

Fig. 1. Schematic diagram of membranes fabrication.

2.4. Analysis of the permeate water samples

The concentration of the target compounds was analyzed using an ultra-performance liquid chromatography (ACQUITY UPLC, Waters Corporation, USA) with ultraviolet detector and fluorescence detector. The mobile phase was consisted of a mixture of acetonitrile and acidified water with 0.1% formic acid. For paracetamol, Ex and Em was missing and the hope Ex was 254nm. E_x 276 nm and E_m 447 nm for norfloxacin, and E_x 280 nm and E_m 360 nm for sulfamethoxazole. The chromatographic column temperature was 35°C and sample temperature was 30°C.

2.5. Permeation performance

The filtration experiments were performed using a cross-flow system. The cross-flow membrane cell was custom-built with an effective membrane area of 46.07 cm². The schematic representation of the experimental set-up is shown in Fig. 2. A 3 L vessel was used as the feed tank, and the feed solution was pumped into the membrane cell via a gear pump (Longer Pump, WT3000-1JB). 2000 mg/L aqueous NaCl and $MgSO_4$ solution was used as feed solution for desalination study and the experiments were carried out at 6 bar (gauge) and ambient temperature. The membranes were compacted at 6 bar with the feed solution of DI water for 1 h to obtain a stable flux prior to testing. The flux was calculated using the following Eq. (1):

$$J = \frac{V}{S \times t} \qquad (1)$$

where *J* is the flux (L m⁻²h⁻¹), *V* is the permeate volume (L), *S* is the membrane effective area (m²), and *t* is the time (h).

In these experiments, the feed solution containing paracetamol, norfloxacin and sulfamethoxazole with concentration of 1 mg/L (pH 6.78) was used for evaluating the PPCPs removal efficiency of the PA/GO TFC membrane. The filtration experiment was carried out for 3 h and the permeate flow was collected every 20 min for analysis.

3. Results and discussion

3.1. Chemical composition of membrane

Four series of TFC membranes with different GO loadings in the semi-aromatic PA active layer (0, 0.004, 0.008 and 0.016 wt%) were fabricated via the IP reaction on the top of commercial PSf UF membranes. These samples were labeled PA/GO-0, PA/GO-4, PA/GO-8, and PA/GO-16, respectively.

The PA layer was form via the reaction between amine groups in PIP and acylchloride groups in TMC. When GO was incorporated into the PA layer, the carboxyl or hydroxyl groups in GO can interact with the acylchloride in TMC, and then form anhydride or ester bond [18].

The chemical structures of membranes were characterized by ATR-FTIR. Fig. 3 presents a comparison of the FTIR spectra of the pristine PSf, PA/GO-0 and PA/GO-16 membranes (ranging from 4000 cm⁻¹ to 800 cm⁻¹). As shown in Fig. 3, the peaks at 1587, 1504, and 1488 cm⁻¹ were clearly observed, which was attributed to the aromatic in-plane ring bend stretching vibration of the PSf membrane [34]. In addition, the asymmetric and symmetric SO_2 stretching vibrations of PSf contributed to the absorption peaks at 1350–1280 cm⁻¹ [34] and 1180–1145 cm⁻¹ [7], respectively. A significant peak at 1245 cm⁻¹ was clearly observed, which was ascribed to the C–O–C asymmetric stretching vibration of the aryl–O–aryl group of PSf [35]. The characteristic absorption peak at 1627 cm⁻¹ was observed for the prepared poly(piperazinamide) membranes and the C–N stretching vibration of the polyamide group appears at 1570 cm⁻¹, which was consistent with the absence of amide II and aromatic amide bands owing to the absence of N–H bond in poly(piperazinamide) and the lack of aromaticity of the amine monomers [7,36]. Compared to the PA membrane without GO, the more significant peak at 3387 cm⁻¹ in the case of GO modified PA membrane was mainly due to the hydroxyl stretching vibration. The presence of hydroxyl groups suggested that the addition of GO could potentially improve the hydrophilicity of the membrane, which was later confirmed by the water filtration tests and water contact angle measurements.

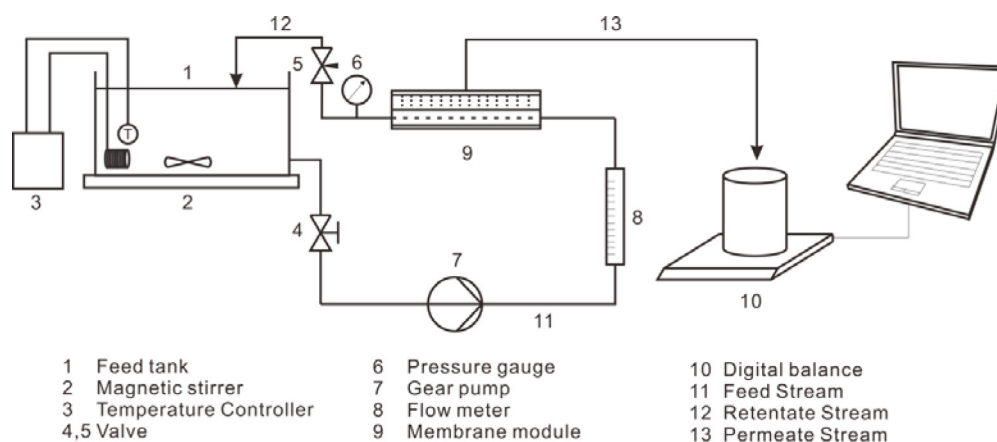| 1 | Feed tank | 6 | Pressure gauge | 10 | Digital balance |
2	Magnetic stirrer	7	Gear pump	11	Feed Stream
3	Temperature Controller	8	Flow meter	12	Retentate Stream
4,5	Valve	9	Membrane module	13	Permeate Stream

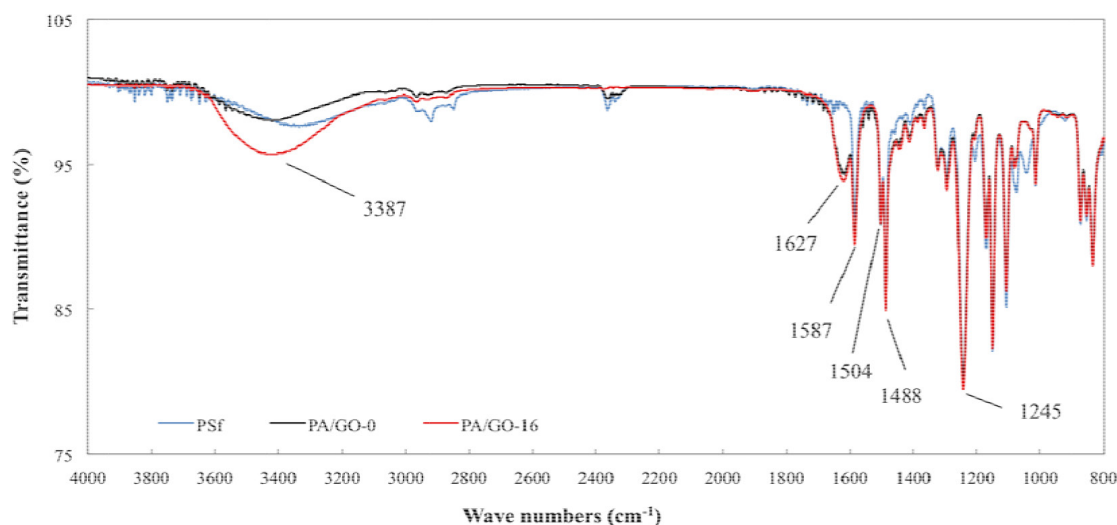Fig. 2. Schematic representation of the bench-scale NF set-up.

Fig. 3. FTIR spectra of PSf and PA TFC membranes.

3.2. Membrane surface morphology

The surface morphology and surface roughness of four TFC membranes were analyzed by scanning electron microscopy (SEM) and atomic force microscopy (AFM). Fig. 4 presents the top surface and cross-sectional SEM images of the TFC membranes with different GO loadings. A rough surface containing grainy nodular structures was found on PA/GO-0 (Fig. 4a), which was a result of cross-linking of PIP and TMC monomers during the IP reaction [14,37]. After embedding GO nano-sheets into the active layer, the size of nodules increased, and some nodules were connected with each other and formed a cross-linked area on the membrane surface (Fig. 4b–d). Moreover, with the increased GO loading, the size of the nodules further increased, and the cross-linked area became larger. At the same time, the membrane surface roughness seemed to be decreased while the surface density increased. In other words, the GO modified TFC membranes have a smoother, denser surface compared to the pure PA TFC membrane. The slower diffusion of PIP in the presence of GO-carboxyl groups resulted in a leaf-like surface. In contrast, a nodular structure was formed according to the fast reaction of PIP with TMC via the IP reaction. Further, it is widely believed that the hydrogen bonding between the polyamide layer and the functional groups of GO composite contributed to a more compact chain structure on the membrane surface with lower surface roughness [38]. Fathizadeh et al. and Kim et al. reported similar results by embedding hydrophilic additives into the polyamide membranes [39,40]. Figs. 4e–f show the cross section SEM images of the pure and GO modified TFC membranes. The cross sections of both membranes possessed a similar structure with the active layer tightly inherent to the PSf support layer. A thinner, denser and smoother active layer was showed in Fig. 4f with embedded GO, which was in line with the surface SEM images (Fig. 4d).

AFM analysis was applied to further investigate the membrane surface roughness. Fig. 5 shows three-dimensional AFM scans of the pure and GO modified TFC membranes with a scan area of 2×2 µm². The surface roughness of GO modified TFC membrane was slightly lower than that of the TFC membranes (R_a = 13.5 nm, R_q = 16.8 nm vs R_a = 16.5 nm, R_q = 21.2 nm). This observation agreed with the SEM images wherein the PA layer of GO modified TFC membranes were smoother, thinner and denser.

3.3. Membrane surface hydrophilicity

Water contact angle was commonly used to assess the membrane hydrophilicity. In Fig. 6, the GO modified TFC membranes appeared to have lower contact angle (PA/GO-0: 60.82 ± 0.72° and PA/GO-16: 49.31 ± 0.40°), which indicated better hydrophilicity with the incorporation of GO. Notably, with the increased loading of GO, the contact angle consistently decreased. At the same time, the PA/GO-16 membrane had a higher value of carboxyl group density (27.67 ± 4.28 nm⁻² vs 20.19 ± 5.83 nm⁻²) compared to that of the PA/GO-0 membrane, which in return emphasizing that the GO modified membrane possessed higher hydrophilicity. The improved membrane hydrophilicity might be attribute to the presence of oxygen-containing functional groups and the correspondingly superior hydrophilicity of GO nano-composite [20,41]. By introducing these hydrophilic additives in the membrane structure, the hydrophilicity of the resultant TFC membranes also increased, and their contact angle decreased correspondingly.

3.4. Zeta potential of membrane

As shown in Fig. 7, the surface charge of the pure PA TFC membrane and GO modified PA TFC membranes were assessed. The zeta potential of PA/GO-0 membrane was −0.92 ± 0.41 mV at pH 6. With the increased GO loadings from 0 to 0.016 wt%, the zeta potential continued to decrease (PA/GO-4: −9.49 ± 0.37 mV, PA/GO-8: −20.87 ± 0.29 mV, PA/GO-16: −25.02 ± 0.36 mV at pH 6). The addition of GO induced a surface negative charge, owing to
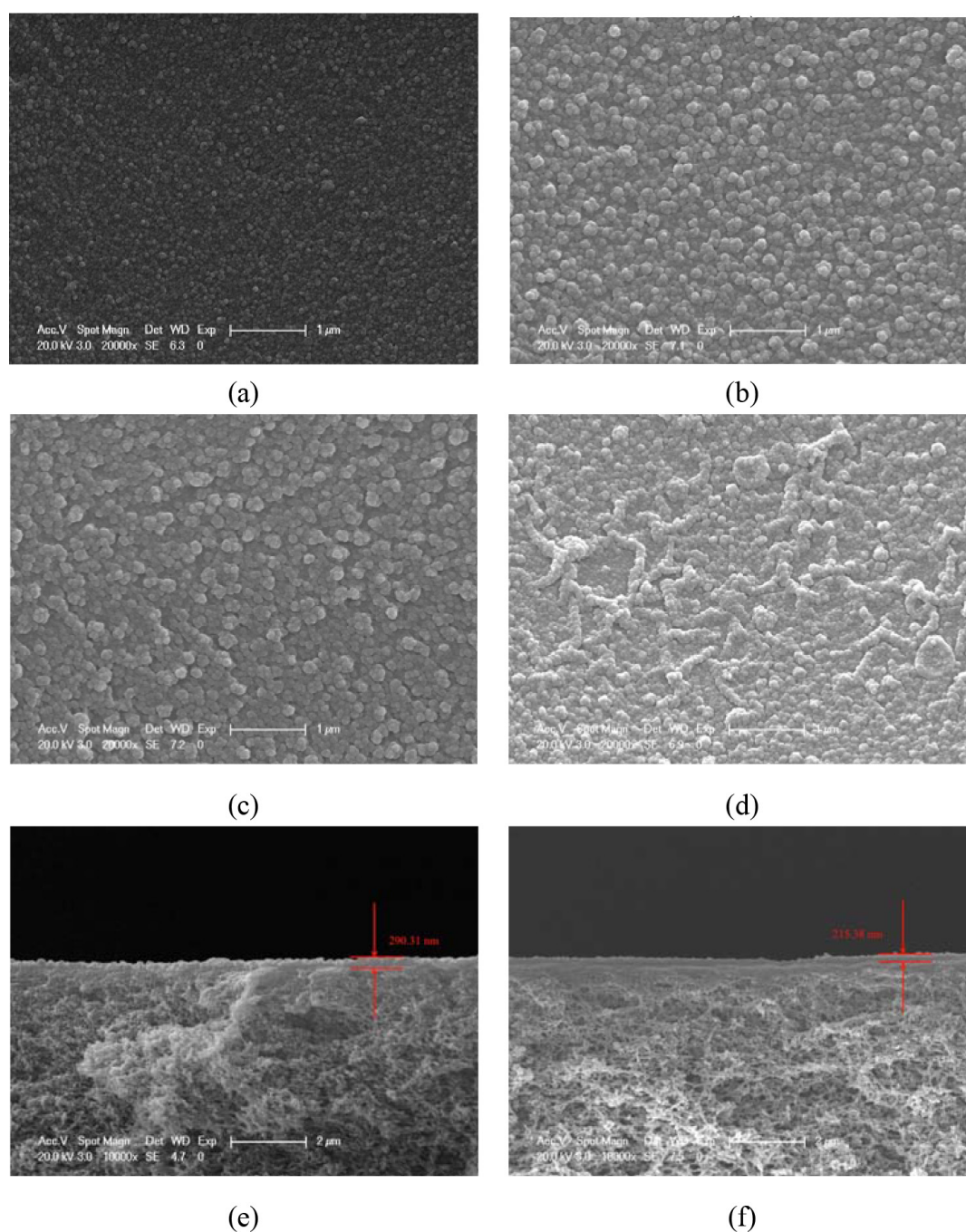
Fig. 4. SEM images of the top surfaces of: (a) PA/GO-0, (b) PA/GO-4, (c) PA/GO-8, and (d) PA/GO-16, and the cross-sections of: (e) PA/GO-0, and (f) PA/GO-16.

the oxygen functional groups of the GO. Furthermore, the membrane with higher GO loadings exhibited a more negative surface charge at higher pH, which was ascribed to the presence of carboxylic groups and their subsequent deprotonation [42,43].

3.5. Water flux and salt rejection

The effect of GO on flux performance was presented in Fig. 8. As shown in Fig. 8, the flux for PA/GO-16 membrane reached 12.78 ± 0.36 L m^{-2} h^{-1} bar^{-1}, an almost 45% improvement in permeability than the pristine PA membrane (PA/GO-0: 8.94 ± 0.42 L m^{-2} h^{-1} bar^{-1}). The significantly improved flux with the incorporation of GO was correspondingly related to the higher membrane hydrophilicity, which might be attributed to its higher affinity to water, hydrolysis with hydroxyl groups and the presence of hydrophilic functional groups of GO.

The membrane separation performance is shown in Fig. 9. The permeation flux (Fig. 9a) and salt rejection (Fig.
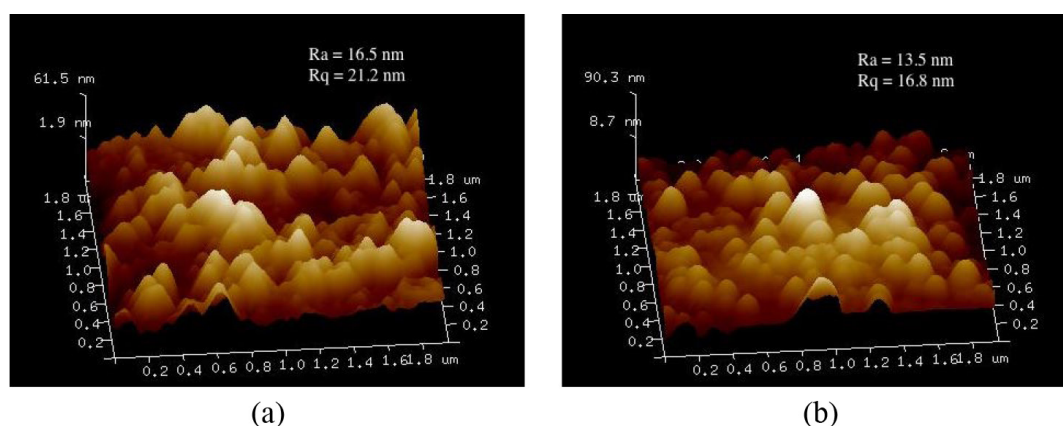
Fig. 5. Three-dimensional AFM images of the surfaces of: (a) PA/GO-0, (b) PA/GO-4.
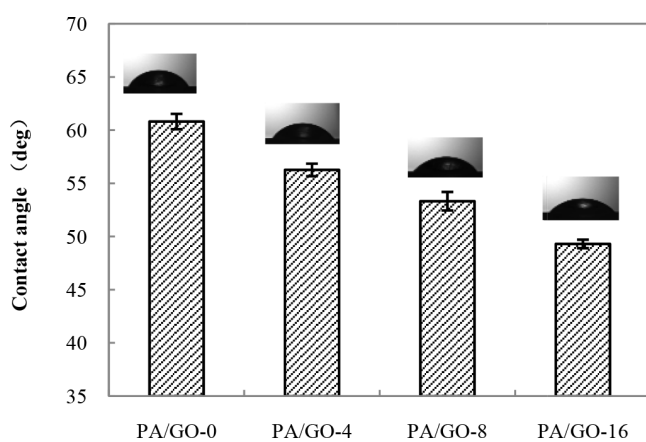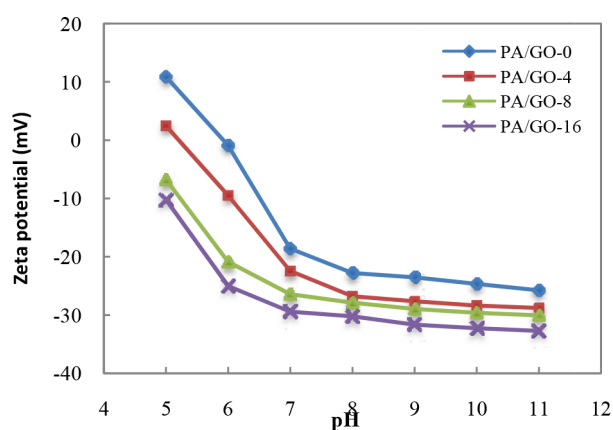

Fig. 6. Water contact angle of the prepared membranes.

Fig. 8. Water flux of the prepared membranes.

Fig. 7. Surface charge over pH range of the prepared membranes.

9b) were tested using 2000 mg/L NaCl and MgSO$_4$ aqueous solution as the feed solution. It can be seen that the GO modified PA TFC membranes exhibited higher flux with similar water flux increment over GO loadings. The relatively lower salt rejection in comparing with the previous research [38] might be ascribed to the fabrication process of membranes. The salt rejection in Fig. 9. indicated
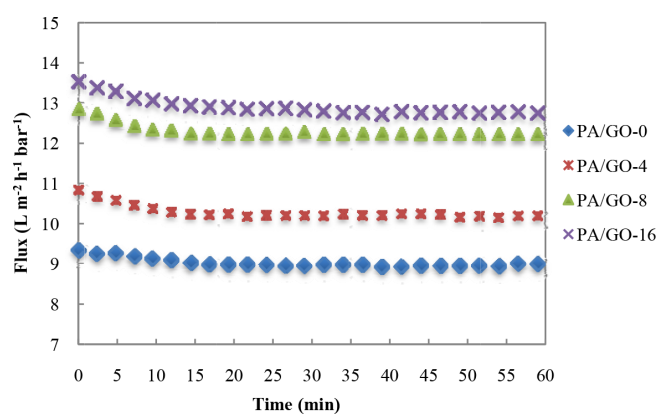
that the TFC membranes showed a low monovalent salt rejection approximately 23.44–25.77%, and a high bivalent salt rejection about 64.88–68.65%. The study of Lo et al. reported that the reaction between m-phenylenediamine (MPD) and TMC for the preparation of TFC membrane offers a much more facile approach compared to the case of PIP and TMC, which can be contributed to the better selectivity of bivalent salt rejection in the later case. The unreacted acyl moieties in piperazine based TFC membranes lead to the change of surface charges, causing the rejection of bivalent counter ions [44]. Compared with the pure PA TFC membrane, the NaCl and MgSO$_4$ rejection of GO modified PA TFC membranes were slightly higher (PA/GO-16: 25.77 ± 0.73% vs PA/GO-0: 23.22 ± 0.34%, PA/GO-16: 68.65 ± 0.47% vs PA/GO-0: 64.88 ± 0.55%). The negative charge of GO-containing membranes has been widely reported in previous studies [45–48] confirming the presence of large numbers of covalent oxygen-containing functional groups—carboxyl, hydroxyl and epoxide in GO. According to Section 3.4, due to the ionization of hydroxyl and carboxyl groups in the GO layers, the GO modified membrane had a negatively charged surface that was more likely to enhance the repulsive electrostatic interactions between the membrane and salt, then achieved higher salt rejection. Generally, the incorporation of GO appeared to achieve better performance than those without GO.
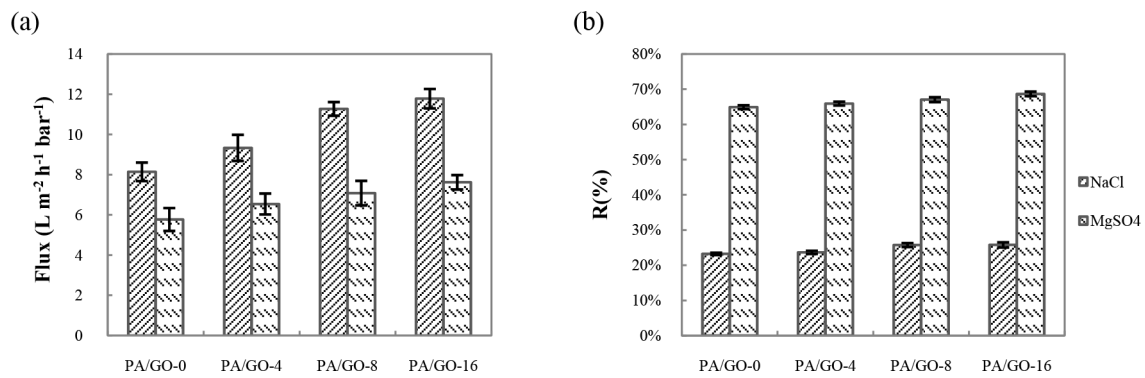
(a)

(b)

Fig. 9. (a) Flux and (b) salt rejection of the prepared membranes.

3.6. PPCPs removal

The normalized water fluxes of pure PA TFC membrane and GO modified PA TFC membranes during the foulant rejection test are shown in Fig. 10a. The flux of both pure PA TFC and GO modified PA TFC membranes slightly decreased within 40 min and then stabilized over time. 6.95, 2.76, 4.63, and 1.11% of water flux declines were observed for PA/GO-0, PA/GO-4, PA/GO-8, and PA/GO-16 membranes, respectively. Meanwhile, the GO modified membranes always maintained higher flux

during the fouling test, indicating better anti-fouling performance with the membrane containing GO, which might be attributed to the higher hydrophilicity that originated from the hydrophilic groups of GO [49]. The surface hydrophilicity can alter the membrane adsorption properties, and thus improving its hydrophilicity and limiting fouling behavior to some extent [26].

Fig. 10b–d shows the effect of the GO loadings on the target PPCPs compound rejection. As shown in Fig. 10b, both pure PA TFC membrane and GO modified PA TFC
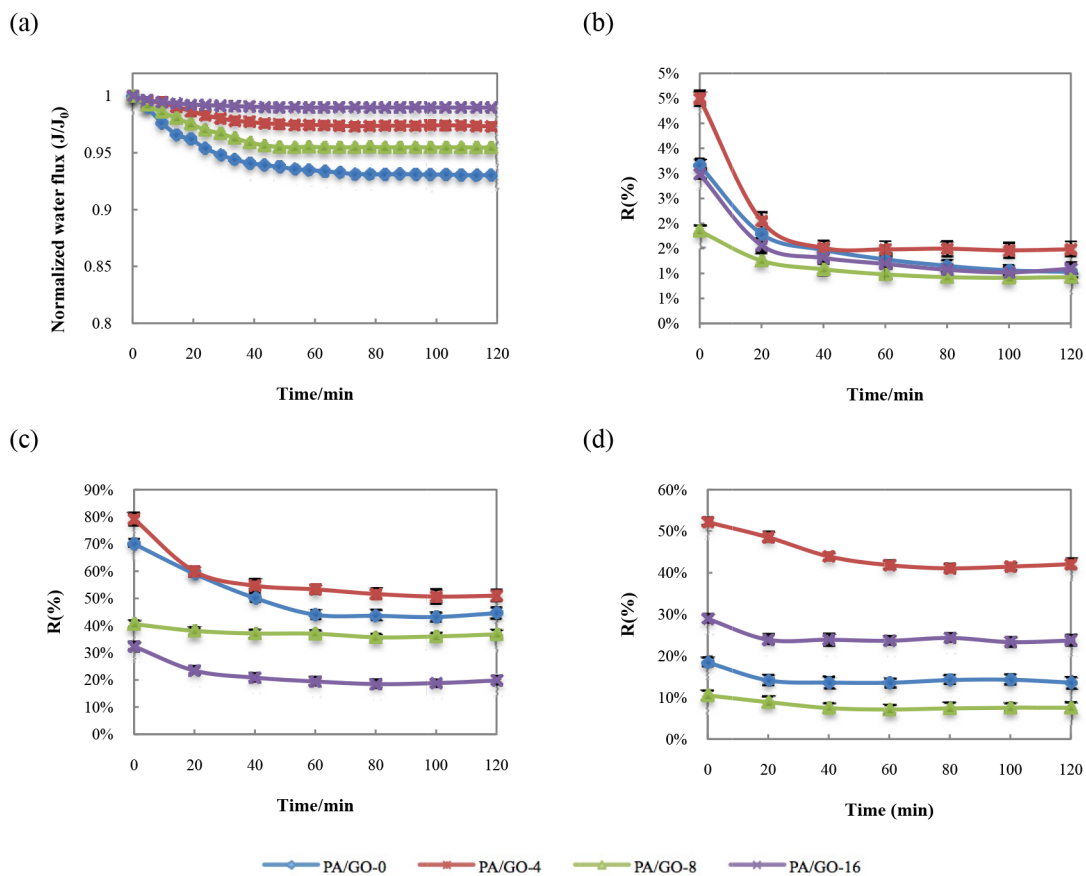
(a)

(b)

(c)

(d)

Fig. 10. (a) Normalized water flux and (b) paracetamol rejection (c) norfloxacin rejection (d) sulfamethoxazole rejection.

membranes had a relatively low paracetamol rejection (<5%), which can be ascribed to its lowest molar weight and highest hydrophilicity resulting from the phenolic group among the three PPCPs. Norfloxacin showed the highest rejection which can be attributed to its highest molar weight among the three PPCPs. In the meantime, the presence of hydrophobic group on norfloxacin also contributed to its higher rejection. In addition, the norfloxacin rejection declined slowly until 40 min and then had a stable performance overt time. The PA/GO-4 membrane had a higher norfloxacin rejection compared to the PA/GO-0 membrane (53.32 ± 1.78% vs. 43.99 ± 1.44% at 60 min), indicating a higher hydrophilicity of the PA/GO-4 membrane, which was consistent with the observation in Section 3.3. However, membrane hydrophilicity increased along with the increased GO loading which resulted in an improved water flux, and subsequently affected the PPCPs rejection to a certain extent. During the 2 h operation time, the sulfamethoxazole rejection was relatively steady. Under the neutral condition, sulfamethoxazole (pKa = 5.7) was predominantly presented as electronegative species. Fig. 10d shows that the PA/GO-4 membrane also exhibited a higher rejection (41.85 ± 1.09% at 60 min) than the PA/GO-0 membrane (13.56 ± 1.02% at 60 min), which can be attributed to the increase in membrane surface negative charge by the embedding of GO (Fig. 7). The electrostatic repulsion between the negatively charged sulfamethoxazole and GO modified PA TFC membrane played a dominant role in their rejection during the fouling test. Nevertheless, PA/GO-16 membrane possesses the highest negative charge while exhibited lower sulfamethoxazole rejection. In the filtering process, PPCPs rejection can be affected by many other factors. The improved water flux of PA/GO-16 membrane will subsequently affect the PPCPs rejection, which may contribute to this phenomenon.

4. Conclusions

In this study, the GO modified semi-aromatic TFC membranes were prepared via the IP reaction on the top of commercial PSf UF membranes. A variety of techniques were applied to characterize the pure PA TFC membrane and GO modified PA TFC membranes. The FE-SEM images of membrane surfaces and cross-sections indicated that the active layer became denser, smoother and thinner due to the incorporation of GO. Meanwhile, the embedding of GO significantly improved the hydrophilicity and negative surface charge of the membranes, which consequently led to a higher pure water flux with slightly improved salt rejection compared to that of the pure PA TFC membranes. In addition, the rejection results of three target PPCPs compounds demonstrated that the incorporation of GO not only led to higher norfloxacin and sulfamethoxazole rejection, but also improved the anti-fouling properties of the membranes.

Acknowledgements

References

[1] P.W. Morgan, Condensation polymers: by interfacial and solution methods, Interscience Publishers, 1965.
[2] M.M. Pendergast, E.M. Hoek, A review of water treatment membrane nanotechnologies, Energy Environ. Sci., 4 (2011) 1946–1971.
[3] W. Lau, S. Gray, T. Matsuura, D. Emadzadeh, J.P. Chen, A. Ismail, A review on polyamide thin film nanocomposite (TFN) membranes: History, applications, challenges and approaches, Water Res., 80 (2015) 306–324.
[4] H.D. Raval, S. Maiti, Ultra-low energy reverse osmosis with thermal energy recovery from photovoltaic panel cooling and TFC RO membrane modification, Desal. Water Treat., 57 (2014) 1–10.
[5] Y. Song, P. Sun, L.L. Henry, B. Sun, Mechanisms of structure and performance controlled thin film composite membrane formation via interfacial polymerization process, J. Membr. Sci., 251 (2005) 67–79.
[6] C.Y. Tang, Q.S. Fu, A. Robertson, C.S. Criddle, J.O. Leckie, Use of reverse osmosis membranes to remove perfluorooctane sulfonate (PFOS) from semiconductor wastewater, Environ. Sci. Technol., 40 (2006) 7343–7349.
[7] C.Y. Tang, Y.-N. Kwon, J.O. Leckie, Effect of membrane chemistry and coating layer on physiochemical properties of thin film composite polyamide RO and NF membranes: I. FTIR and XPS characterization of polyamide and coating layer chemistry, Desalination, 242 (2009) 149–167.
[8] C.Y. Tang, Y.-N. Kwon, J.O. Leckie, Effect of membrane chemistry and coating layer on physiochemical properties of thin film composite polyamide RO and NF membranes: II. Membrane physiochemical properties and their dependence on polyamide and coating layers, Desalination, 242 (2009) 168–182.
[9] N. Saha, S. Joshi, Performance evaluation of thin film composite polyamide nanofiltration membrane with variation in monomer type, J. Membr. Sci., 342 (2009) 60–69.
[10] Y. Li, Y. Su, Y. Dong, X. Zhao, Z. Jiang, R. Zhang, J. Zhao, Separation performance of thin-film composite nanofiltration membrane through interfacial polymerization using different amine monomers, Desalination, 333 (2014) 59–65.
[11] Y. Mansourpanah, S. Madaeni, A. Rahimpour, Fabrication and development of interfacial polymerized thin-film composite nanofiltration membrane using different surfactants in organic phase; study of morphology and performance, J. Membr. Sci., 343 (2009) 219–228.
[12] A.H.M.A. El-Aassar, Improvement of reverse osmosis performance of polyamide thin-film composite membranes using TiO₂ nanoparticles, Desal. Water Treat., 55 (2014) 1–12.
[13] S. Liu, M. Zhang, F. Fang, L. Cui, J. Wu, R. Field, K. Zhang, Biogenic silver nanocomposite TFC nanofiltration membrane with antifouling properties, Desal. Water Treat., 30 (2015) 1–12.
[14] J.N. Shen, C.C. Yu, H.M. Ruan, C.J. Gao, B.V. Bruggen, Preparation and characterization of thin-film nanocomposite membranes embedded with poly (methyl methacrylate) hydrophobic modified multiwalled carbon nanotubes by interfacial polymerization, J. Membr. Sci., 442 (2013) 18–26.
[15] S. Xia, L. Yao, Y. Zhao, N. Li, Y. Zheng, Preparation of graphene oxide modified polyamide thin film composite membranes with improved hydrophilicity for natural organic matter removal, Chem. Eng. J., 280 (2015) 720–727.
[16] B. Mi, Graphene oxide membranes for ionic and molecular sieving, Science, 343 (2014) 740–742.
[17] C. Xu, A. Cui, Y. Xu, X. Fu, Graphene oxide–TiO₂ composite filtration membranes and their potential application for water purification, Carbon, 62 (2013) 465–471.
[18] M. Hu, B. Mi, Enabling graphene oxide nanosheets as water separation membranes, Environ. Sci. Technol., 47 (2013) 3715–3723.
[19] R. Joshi, P. Carbone, F. Wang, V. Kravets, Y. Su, I. Grigorieva, H. Wu, A. Geim, R. Nair, Precise and ultrafast molecular sieving through graphene oxide membranes, Science, 343 (2014) 752–754.

[20] J. Lee, H.-R. Chae, Y.J. Won, K. Lee, C.-H. Lee, H.H. Lee, I.-C. Kim, J.-m. Lee, Graphene oxide nanoplatelets composite membrane with hydrophilic and antifouling properties for wastewater treatment, J. Membr. Sci., 448 (2013) 223–230.

[21] F. Perreault, M.E. Tousley, M. Elimelech, Thin-film composite polyamide membranes functionalized with biocidal graphene oxide nanosheets, Environ. Sci. Technol. Lett., 1 (2013) 71–76.

[22] H.M. Hegab, L. Zou, Graphene oxide-assisted membranes: Fabrication and potential applications in desalination and water purification, J. Membr. Sci., 484 (2015) 95–106.

[23] D.A. Dikin, S. Stankovich, E.J. Zimney, R.D. Piner, G.H. Dommett, G. Evmenenko, S.T. Nguyen, R.S. Ruoff, Preparation and characterization of graphene oxide paper, Nature, 448 (2007) 457–460.

[24] M. Koinuma, C. Ogata, Y. Kamei, K. Hatakeyama, H. Tateishi, Y. Watanabe, T. Taniguchi, K. Gezuhara, S. Hayami, A. Funatsu, Photochemical engineering of graphene oxide nanosheets, J. Phys. Chem., C116 (2012) 19822–19827.

[25] H.J. Kim, M.-Y. Lim, K.H. Jung, D.-G. Kim, J.-C. Lee, High-performance reverse osmosis nanocomposite membranes containing the mixture of carbon nanotubes and graphene oxides, J. Mater. Chem. A., 3 (2015) 6798–6809.

[26] S. Bano, A. Mahmood, S.-J. Kim, K.-H. Lee, Graphene oxide modified polyamide nanofiltration membrane with improved flux and antifouling properties, J. Mater. Chem. A., 3 (2015) 2065–2071.

[27] T.A. Ternes, A. Joss, H. Siegrist, Peer reviewed: scrutinizing pharmaceuticals and personal care products in wastewater treatment, Environ. Sci. Technol., 38 (2004) 392A–399A.

[28] L.D. Nghiem, A.I. Schfer, M. Elimelech, Pharmaceutical retention mechanisms by nanofiltration membranes, Environ. Sci. Technol., 39 (2005) 7698–7705.

[29] Y. Yoon, P. Westerhoff, S.A. Snyder, E.C. Wert, J. Yoon, Removal of endocrine disrupting compounds and pharmaceuticals by nanofiltration and ultrafiltration membranes, Desalination, 202 (2007) 16–23.

[30] H. Ozaki, N. Ikejima, Y. Shimizu, K. Fukami, S. Taniguchi, R. Takanami, R. Giri, S. Matsui, Rejection of pharmaceuticals and personal care products (PPCPs) and endocrine disrupting chemicals (EDCs) by low pressure reverse osmosis membranes, Water Sci. Technol., 58 (2008) 73.

[31] M.A. Zazouli, H. Susanto, S. Nasseri, M. Ulbricht, Influences of solution chemistry and polymeric natural organic matter on the removal of aquatic pharmaceutical residuals by nanofiltration, Water Res., 43 (2009) 3270–3280.

[32] E.-E. Chang, Y.-C. Chang, C.-H. Liang, C.-P. Huang, P.-C. Chiang, Identifying the rejection mechanism for nanofiltration membranes fouled by humic acid and calcium ions exemplified by acetaminophen, sulfamethoxazole, and triclosan, J. Hazard. Mater., 221 (2012) 19–27.

[33] A. Tiraferri, M. Elimelech, Direct quantification of negatively charged functional groups on membrane surfaces, J. Membr. Sci., 389 (2012) 499–508.

[34] Y.-N. Kwon, J.O. Leckie, Hypochlorite degradation of crosslinked polyamide membranes: II. Changes in hydrogen bonding behavior and performance, J. Membr. Sci., 282 (2006) 456–464.

[35] S.R. Laboratories, The Infrared spectra atlas of monomers and polymers, Sadtler Research Laboratories, 1980.

[36] Q. Li, Y. Wang, J. Song, Y. Guan, H. Yu, X. Pan, F. Wu, M. Zhang, Influence of silica nanospheres on the separation performance of thin film composite poly (piperazine-amide) nanofiltration membranes, Appl. Surf. Sci., 324 (2015) 757–764.

[37] R.J. Petersen, Composite reverse osmosis and nanofiltration membranes, J. Membr. Sci., 83 (1993) 81–150.

[38] M. Safarpour, V. Vatanpour, A. Khataee, M. Esmaeili, Development of a novel high flux and fouling-resistant thin film composite nanofiltration membrane by embedding reduced graphene oxide/TiO$_2$, Sep. Purif. Technol., 154 (2015) 96–107.

[39] M. Fathizadeh, A. Aroujalian, A. Raisi, Effect of added NaX nano-zeolite into polyamide as a top thin layer of membrane on water flux and salt rejection in a reverse osmosis process, J. Membr. Sci., 375 (2011) 88–95.

[40] S.H. Kim, S.-Y. Kwak, B.-H. Sohn, T.H. Park, Design of TiO$_2$ nanoparticle self-assembled aromatic polyamide thin-film-composite (TFC) membrane as an approach to solve biofouling problem, J. Membr. Sci., 211 (2003) 157–165.

[41] M. Safarpour, A. Khataee, V. Vatanpour, Preparation of a novel polyvinylidene fluoride (PVDF) ultrafiltration membrane modified with reduced graphene oxide/titanium dioxide (TiO$_2$) nanocomposite with enhanced hydrophilicity and antifouling properties, Ind. Eng. Chem. Res., 53 (2014) 13370–13382.

[42] J. Yin, E.-S. Kim, J. Yang, B. Deng, Fabrication of a novel thin-film nanocomposite (TFN) membrane containing MCM-41 silica nanoparticles (NPs) for water purification, J. Membr. Sci., 423 (2012) 238–246.

[43] T. Szabó, E. Tombácz, E. Illés, I. Dékány, Enhanced acidity and pH-dependent surface charge characterization of successively oxidized graphite oxides, Carbon, 44 (2006) 537–545.

[44] R. Lo, A. Bhattacharya, B. Ganguly, Probing the selective salt rejection behavior of thin film composite membranes: A DFT study, J. Membr. Sci., 436 (2013) 90–96.

[45] B. Ganesh, A.M. Isloor, A.F. Ismail, Enhanced hydrophilicity and salt rejection study of graphene oxide-polysulfone mixed matrix membrane, Desalination, 313 (2013) 199–207.

[46] H. Zhao, L. Wu, Z. Zhou, L. Zhang, H. Chen, Improving the antifouling property of polysulfone ultrafiltration membrane by incorporation of isocyanate-treated graphene oxide, Phys. Chem. Chem. Phys. 15 (2013) 9084–9092.

[47] J. Zhang, Z. Xu, M. Shan, B. Zhou, Y. Li, B. Li, J. Niu, X. Qian, Synergetic effects of oxidized carbon nanotubes and graphene oxide on fouling control and anti-fouling mechanism of polyvinylidene fluoride ultrafiltration membranes, J. Membr. Sci., 448 (2013) 81–92.

[48] X. Zhang, C. Cheng, J. Zhao, L. Ma, S. Sun, C. Zhao, Polyethersulfone enwrapped graphene oxide porous particles for water treatment, Chem. Eng. J., 215 (2013) 72–81.

[49] Z. Wang, H. Yu, J. Xia, F. Zhang, F. Li, Y. Xia, Y. Li, Novel GO-blended PVDF ultrafiltration membranes, Desalination, 299 (2012) 50–54.